Molecular Crystals and Liquid Crystals

Publication details, including instructions for authors and subscription information:
http://www.tandfonline.com/loi/gmcl20

Photoresponsive and Holographic Behavior of an Azobenzene-Containing Block Copolymer and a Random Copolymer

Yumiko Naka [a], Haifeng Yu [a], Atsushi Shishido [a] & Tomiki Ikeda [a]

[a] Chemical Resources Laboratory, Tokyo Institute of Technology, Yokohama, Japan

Version of record first published: 22 Jul 2010

To cite this article: Yumiko Naka, Haifeng Yu, Atsushi Shishido & Tomiki Ikeda (2009): Photoresponsive and Holographic Behavior of an Azobenzene-Containing Block Copolymer and a Random Copolymer, Molecular Crystals and Liquid Crystals, 498:1, 118-130

To link to this article: http://dx.doi.org/10.1080/15421400802615105

Mol. Cryst. Liq. Cryst., Vol. 498, pp. 118–130, 2009

ISSN: 1542-1406 print/1563-5287 online
DOI: 10.1080/15421400802615105

Taylor & Francis
Taylor & Francis Group

Photoresponsive and Holographic Behavior of an Azobenzene-Containing Block Copolymer and a Random Copolymer

Yumiko Naka, Haifeng Yu, Atsushi Shishido, and Tomiki Ikeda
Chemical Resources Laboratory, Tokyo Institute of Technology, Yokohama, Japan

A block copolymer containing an azobenzene (Az) moiety in the side chain was prepared by atom transfer radical polymerization (ATRP). For comparison, a random copolymer with a similar Az content was also designed. Their photoresponsive and holographic behavior was investigated in thin films. The block copolymer film showed microphase separation with cylinder microdomains after annealing, which was then irradiated at 366 nm. It was found that trans-cis *photoisomerization in the block copolymer film was slower than that in the random copolymer film. This may be due to the restricted motion of the Az moieties in the Az blocks. The photoinduced birefringence (Δn) of the block copolymer film was higher than that of the random copolymer film upon irradiation with a linearly polarized beam. In holographic recording, similar results were obtained. A block copolymer with 22-mol% Az showed a liquid-crystalline (LC) phase, while a random copolymer with 24-mol% Az exhibited no LC phase. The block copolymer showed an LC phase at a lower Az content compared with the random copolymer, suggesting that the molecular alignment of Az mesogenic groups is enhanced by cooperative motion of LCs in block copolymer films.*

Keywords: atom transfer radical polymerization (ATRP); azobenzene; block copolymer; holography

INTRODUCTION

As information technology has developed, advanced recording media are expected with quick data transfer and high density. Holography provides unique opportunities for the next-generation storage

Address correspondence to Tomiki Ikeda, Chemical Resources Laboratory, Tokyo Institute of Technology, R1-11, 4259 Nagatsuta, Midori-ku, Yokohama 226-8503, Japan. E-mail: tikeda@res.titech.ac.jp

technique. It is well known that the basis in the storage process is a photoinduced change in refractive index in materials with chromophores. This process can be easily achieved in azobenzene (Az)-containing polymers by photoinduced changes in alignment of Az moieties [1,2], which has been widely used in holograms [3,4].

Previously, we reported the formation of holographic gratings in thick films by modulation of refractive index ($\Delta n'$), which can be induced by the change in alignment of Az moieties and mesogens such as cyanobiphenyl or tolane moieties [5,6]. The random copolymers showed the maximum diffraction efficiency of 97% in the Bragg regime. In addition, 55 holograms with angular multiplicity were successfully recorded. On the other hand, Wendorff *et al*. performed the recording of birefringence gratings by Az LC polymers [4]. The LC polymers with Az moieties in the side chain are expected to have a higher degree of anisotropy than amorphous ones. However, the LC polymers have to be aligned by external fields such as an electric field, light, or rubbing treatment.

Block copolymers self-assemble in the process of microphase separation [7–18]. Zhao *et al*. reported that the interfacial interaction between polystyrene and Az groups might control the motion of Az moieties [19,20]. Seki *et al*. reported that the nanostructure formed in block copolymers with poly(ethylene oxide) (PEO) was controlled by the film thickness [21]. The block copolymers have LC continuous phases. Films with low absorption and small scattering of visible light are ideal for volume holograms, which might be obtained by nanoscale phase separation of block copolymer films with LC dispersed phases.

The formation of holographic gratings in thick films was studied by Minabe *et al.* and Häckel *et al.* by blending the block copolymers with homopolymers [7,8,22]. The microphase separation may obtain high arrangement of mesogens by the cooperative effect of LCs in a microphase-separated structure. However, they did not compare these properties between block copolymers and random ones.

In this paper, an Az-containing block copolymer was prepared by an atom transfer radical polymerization (ATRP) method, and its photoisomerization, photoalignment and holographic properties were investigated.

EXPERIMENTAL

Synthesis of Polymers

As shown in Scheme 1, poly(methyl methacrylate) (PMMA) macroinitiator (**PMMA-Br**) was prepared by ATRP in a Pyrex tube ampoule [23]. After MMA (5.0 g, 50 mmol), Cu(I)Cl (0.15 g, 15 mmol),

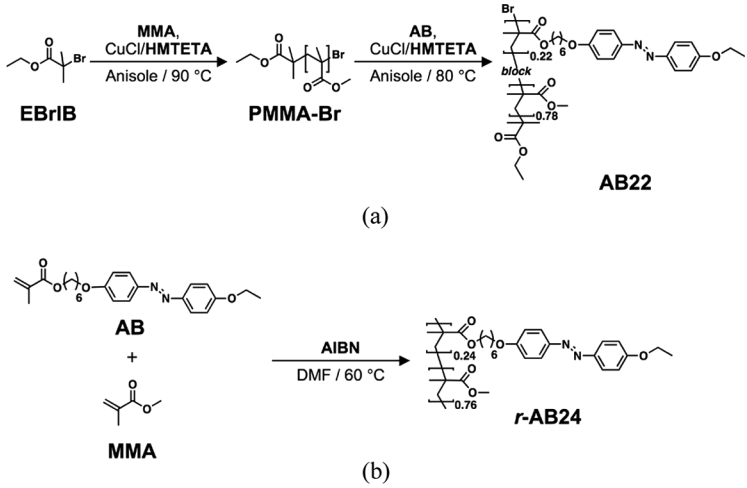

SCHEME 1 Synthetic routes of **AB22** and ***r*-AB24** used in this study.

1,1,4,7,10,10-hexamethyltriethlyenetetramine (**HMTETA**, 420 μL, 15 mmol), ethyl-2-bromoisobutyrate (EBrIB, 73 μL, 0.5 mmol) and anisole (50 mL) were mixed, the mixture was degassed using freeze-pomp-thaw cycles and sealed under vacuum, then stirred for 30 min at room temperature. The reaction was carried out in a preheated oil bath at 90°C for 35 min. Then the ampoule tube was opened and quickly cooled in an ice bath. The polymer solution was passed through a column (silica gel) with THF as eluent to remove the catalyst, and **PMMA-Br** was precipitated in a large excess of methanol and finally dried under vacuum. A white solid product was obtained with a yield of 95%.

Then the bromo-terminated PMMA (**PMMA-Br**) was used as a macroinitiator to synthesize the Az-containing diblock copolymer by ATRP. **PMMA-Br**, Cu(I)Cl and (6-[4-(4-ethoxyphenylazo)phenoxy] hexyl methacrylate were mixed in a 20 mL ampoule that was degassed, filled with argon and put in an argon-filled glove box. Then **HMTETA** and anisole were added. The mixture was sealed under argon and then placed in an oil bath preheated at 80°C for 40 h. After polymerization, the polymer was purified as mentioned above. The obtained block copolymer contained 22-mol% Az calculated from UV-vis absorption spectra, which is abbreviated as **AB22**.

For comparison, a random copolymer with almost the same content of Az as that in **AB22** was also prepared. Polymerization was conducted in *N*,*N*-dimethylformamide (DMF) by using 2,2′-azobis(isobutyronitrile)

(AIBN) as an initiator. The monomer mixture was copolymerized under vacuum at 60°C for 48 h. Then the solution was poured into methanol with stirring to precipitate the polymer. The obtained polymer was purified by precipitation from THF into a large excess of methanol and finally dried under vacuum. This polymer contained 24-mol% Az moieties, which is abbreviated as ***r*-AB24**.

The molecular weight of polymers was determined by gel permeation chromatography (GPC; Japan Spectroscopy Co., model DG-980-50; column, Shodex GPC K802 + K804 + K805; eluent, chloroform) using standard polystyrenes for calibration. The thermodynamic properties of polymers were analyzed with a differential scanning calorimeter (DSC, Seiko I&E SSC-5200 and DSC220C) at heating and cooling rate of 10°C/min. At least three scans were performed to check the reproducibility. The mole fraction of the Az moiety in the copolymers was estimated by the absorbance of the copolymers and the monomers in toluene measured by UV-vis spectroscopy (JASCO, V-550). Atomic force microscopy (AFM) images of surface modulation were detected with a scanning probe microscope (Veeco Instruments Inc., Nanoscope IV) in a tapping mode at room temperature.

Film Preparation

The **AB22** films with a thickness of 100–230 nm were prepared by spin-coating their toluene solution on glass substrates. The films were annealed at 140°C in a vacuum oven for 40 h. The heating and cooling rates were controlled at 0.5°C/min and 0.1°C/min, respectively.

Optical Setup

The optical setup for the evaluation of the photoinduced birefringence in films is shown in Figure 1(a). The polymer film was irradiated with a 488 nm *s*-polarized beam from an Ar^+ laser (Spectra Physics, Inc., BeamLok2065-7S) at 100 mW/cm^2. The intensity of a probe beam at 633 nm from a He-Ne laser (NEC, Co., GLS5370) transmitted through a pair of crossed polarizers, with the sample film between them, was measured with a photodiode. The photoinduced birefringence (Δn) was estimated from the change in transmittance by Eq. (1),

$$T = \sin^2\left(\frac{\pi d \Delta n}{\lambda}\right) \tag{1}$$

where d is the film thickness and λ is the wavelength of the probe beam, respectively. All experiments were carried out at room

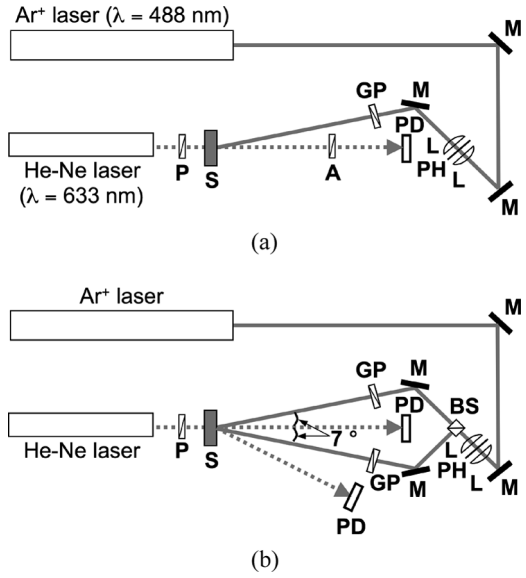

FIGURE 1 Optical setup for the evaluation of the photoinduced birefringence (Δn) (a) and the formation of gratings (b). A, analyzer; BS, beam splitter; GP, Glan-Thomson prisms; L, lens; M, mirror; PH, pinhole; S, sample; P, polarizer; PD, photodiode.

temperature. Figure 1(b) illustrates the optical setup for the grating recording. The two linearly *s*-polarized beams at 488 nm obtained with a beam splitter at an equal intensity were interfered on a film at an incident angle of 7°. The total intensity of the writing beams was adjusted at 100 mW/cm^2. The grating formation was evaluated by monitoring the first-order diffraction beam (I_1) at 633 nm from a He-Ne laser with a photodiode in real time. The first-order diffraction efficiency (η) was defined as the ratio of I_1 to the intensity of the transmitted beam before recording (I_0).

$$\eta = \frac{I_1}{I_0} \tag{2}$$

In this study, all the experiments were performed in the Raman-Nath (thin) regime. Modulation of refractive index ($\Delta n'$) between the bright and dark fringes of the interference pattern was estimated by Eq. (3), assuming that the diffraction is due to the change in the refractive index alone,

$$\eta = \left(\frac{\pi \Delta n' d}{\lambda}\right)^2 \tag{3}$$

where d is the film thickness and λ is the wavelength of the probe beam, respectively.

RESULTS AND DISCUSSION

Properties of Polymers

Both **PMMA-Br** and **AB22** with low polydispersities of 1.12 and 1.06 were successfully prepared, respectively. **AB22** showed an LC phase between 94°C and 147°C, while ***r*-AB24** was amorphous. This suggests that the block copolymer can exhibit an LC phase in a lower concentration of Az mesogens than the random copolymer because of the existence of mesogens in the neighborhood.

Upon annealing at 140°C, cylinder structures were formed by self-assembly in the **AB22** film. The nanostructures of the surface and the cross section of the film were explored by AFM in a tapping mode. As shown in Figure 2, the **AB22** film showed a fingerprint-like structure, with Az LC cylinders irregularity dispersed in the PMMA matrix in the surface (Fig. 2(a)) and dots in the cross section (Fig. 2(b)). The cylinders might be orientated parallel to the substrate plane owing to the thin thickness.

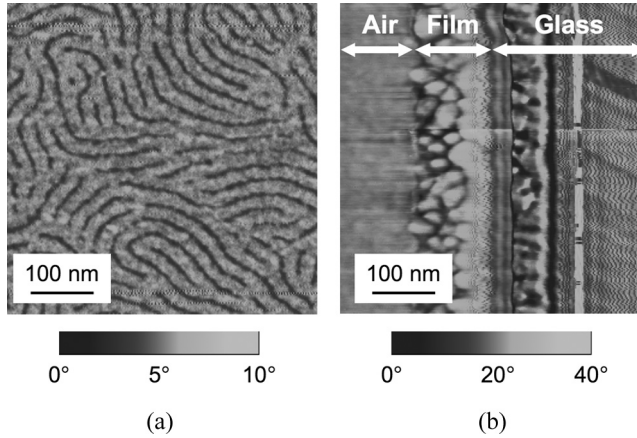

FIGURE 2 AFM phase image of **AB22** film after annealing at 140°C. Surface (a) and cross section (b).

Effect of Microphase Separation on *trans-cis* Photoisomerization and *cis-trans* Thermal Isomerization Behavior

To study the effect of microphase separation on the photoisomerization behavior of **AB22** and ***r*-AB24**, UV-vis spectra were measured in both solution and film as shown in Figure 3. The maximum absorption band at 360 nm was observed in the UV-vis spectra of the copolymers in toluene, owing to the π-π^* transition of Az chromophores. The absorption band of **AB22** was the same as that of ***r*-AB24** in toluene (Figs. 3(a) and (b)). However, as shown in Figure 3(c), a broad spectrum of the absorption band was obtained in the **AB22** films after annealing. Generally, Az chromophores form aggregates in films. The H- and J-aggregates are formed in films, whose absorption peaks are shifted toward shorter and longer wavelengths, respectively. It was observed in Figure 3(c) that Az moieties formed both H- and J-aggregates in the **AB22** film. In the ***r*-AB24** film (Fig. 3(d)), the absorption spectrum was the same as that in solution (Fig. 3(b)), which indicates that the aggregates were not formed. These results suggest

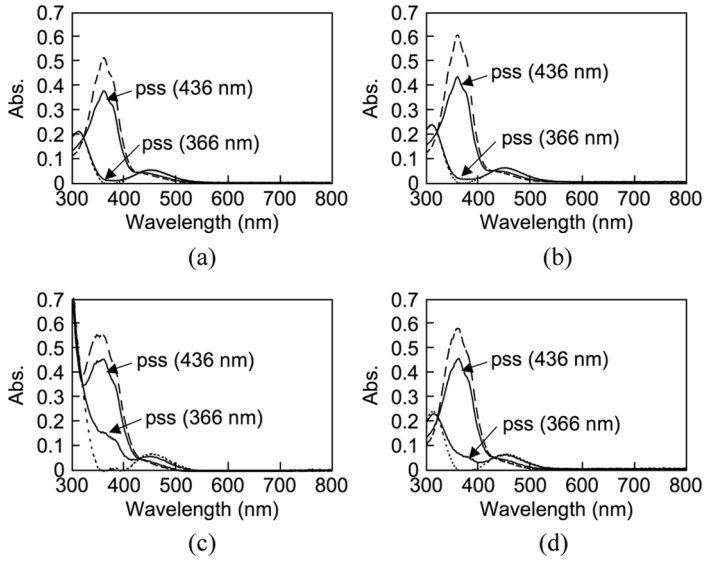

FIGURE 3 UV-vis spectra of **AB22** in toluene (a), ***r*-AB24** in toluene (b), **AB22** in film (c) and ***r*-AB24** in film (d). (Solid line) photostationary state obtained by irradiation at 366 nm and 436 nm; (broken line) *trans*-Az; (doted line) *cis*-Az.

that in the **AB22** film with phase separation, the Az chromophore are located in closer proximity than in the ***r*-AB24** film.

Next we explored *trans-cis* photoisomerization and *cis-trans* thermal isomerization behavior in detail. To obtain absorption spectra of pure *cis*-Az, the Fisher method was employed [24,25]. The absorption spectra of 100% *cis*-Az can be estimated from the absorption spectra of an unirradiated state and two photostationary states achieved by irradiation at two different wavelengths. The absorption spectra in the photostationary states by irradiation at 366 nm and 436 nm from a high-pressure mercury lamp through glass filters (AGC TECHNO GLASS CO., LTD.; 366 nm: UV-35, UV-D36B and IRA-25S; 436 nm: V-40, Y-43 and IRA-25S) are shown in Figure 3 as solid lines. The absorption spectra of 100% *trans*-Az and 100% *cis*-Az estimated by the Fischer method are shown in Figure 3 as broken and doted lines, respectively. Evaluated *cis* ratio in the photostationary state by irradiation at 366 nm was 97% in ***r*-AB24** and **AB22** solution. On the other hand, it was 88% and 72% in ***r*-AB24** and **AB22** films, respectively.

Trans-cis photoisomerization of Az was explored by irradiation of the solution and film of **AB22** and ***r*-AB24** at 366 nm (0.9 mW/cm^2) and 436 nm (1.7 mW/cm^2) until they reached the photostationary states. The photoisomerization behavior was analyzed by the following equation:

$$\ln\left(\frac{A_{\text{trans}} - A_{\text{pss}}}{A_{\text{t}} - A_{\text{pss}}}\right) = k_{\text{tc}}t \tag{4}$$

where A_{t}, A_{trans} and A_{pss} are the absorbance at 360 nm at irradiation time t, of 100% *trans*-Az, and in the photostationary state obtained by irradiation at 366 nm, respectively. The k_{tc} is a rate constant for *trans-cis* photoisomerization. As shown in Figure 4, the photoisomerization of

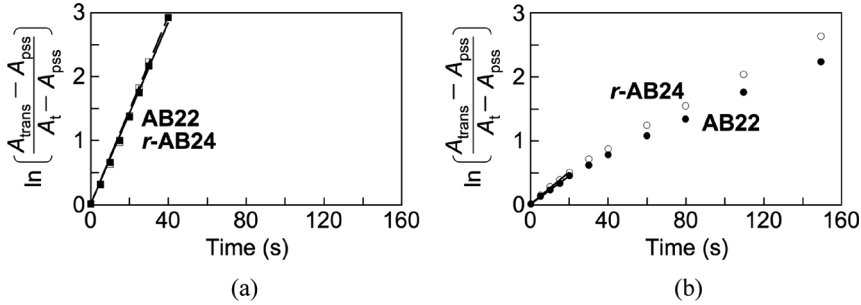

FIGURE 4 First-order plots for *trans-cis* photoisomerization of **AB22** and ***r*-AB24** in toluene (a) in film (b).

Az in toluene could be well described by first-order plots. However, in the films it deviated from the first-order plots. The deviations are reported to result from the lower rate of photoisomerization with an increase in irradiation time, which has been interpreted in terms of a decrease in the number of Az molecules located in sites with free volume enough for photoisomerization [26]. The photoisomerization observed in the **AB22** film was slower than that of the ***r*-AB24** film, in which Az moieties are dispersed homogeneously across the film. The motion of Az moieties may be restricted in the **AB22** film with phase separation. Zhao *et al.* reported that Az moieties were anchored at the interface of microphase separation [22].

The samples were kept in the dark to investigate *cis-trans* thermal isomerization behavior after attainment of the photostationary state at room temperature. The first-order plots according to Eq. (5) for *cis-trans* thermal isomerization of Az are shown in Figure 5,

$$\ln\left(\frac{A_{\text{trans}} - A_{\text{pss}}}{A_{\text{trans}} - A_{\text{t}}}\right) = k_{\text{ct}}t \tag{5}$$

where A_{t}, A_{trans} and A_{pss} are the absorbance at 360 nm at time t in the dark, that of 100% *trans*-Az, and that in the photostationary state obtained by irradiation at 366 nm, respectively. The k_{ct} is the rate constant for thermal *cis-trans* isomerization. The reactions of both **AB22** and **r-AB24** obeyed good first-order kinetics in toluene in the time region observed. However, plots of $\ln[(A_{\text{trans}} - A_{\text{pss}})/(A_{\text{trans}} - A_{\text{t}})]$ *vs.* time showed deviation from a straight line in the films. It might be caused by a steric effect dictated by available free volumes [27,28] and by a matrix effect to trap *cis* isomers in stained conformation upon irradiation at 366 nm [29]. The same results were reported by Mita *et al.* [26].

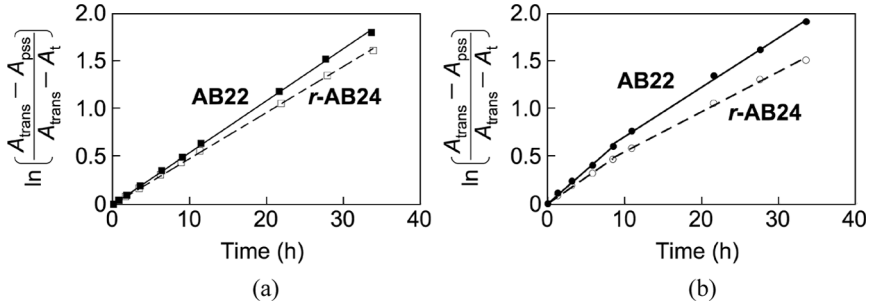

FIGURE 5 First-order plots for thermal *cis-trans* isomerization of **AB22** and ***r*-AB24** in toluene (a) in film (b).

Photoinduced Birefringence and Modulation of Refractive Index

The photoinduced change in Az alignment of **AB22** and ***r*-AB24** was investigated by irradiation with a linearly polarized beam. Upon irradiation, the birefringence increased in both films (Fig. 6), which can be explained by a photoinduced change in alignment of Az moieties with their transition moments almost perpendicular to the polarization direction of the actinic light by repetition of *trans-cis-trans* isomerization cycles. In the ***r*-AB24** film, Δn increased immediately upon irradiation and reached the maximum at about 1 min, while Δn increased slowly in the **AB22** film. Considering the *trans-cis* photoisomerization behavior of Az moieties described in the preceding section, it is reasonable to infer that the change in alignment of Az in the **AB22** film is slower than that in the ***r*-AB24** film. However, the Δn of **AB22** finally reached about 0.14 upon irradiation, which is twice as high as that of ***r*-AB24**. The alignment of Az may be enhanced by cooperative motion of LCs in the **AB22** film, which could lead to a higher Δn.

Then the holographic properties were investigated on the **AB22** and ***r*-AB24** films. Upon irradiation with two linearly polarized beams, the $\Delta n'$ increased, because the difference in the refractive index between the dark and bright fringes becomes larger. Generally, *trans*-Az prefers to be aligned perpendicular to the polarization direction of the actinic beam in the bright area. Further irradiation of the writing beams led to a decay in $\Delta n'$. Figure 7 shows the value of $\Delta n'$ estimated from η as a function of exposure time for the **AB22** and ***r*-AB24** films. The maximum value of $\Delta n'$ was achieved in the **AB22** film, which is

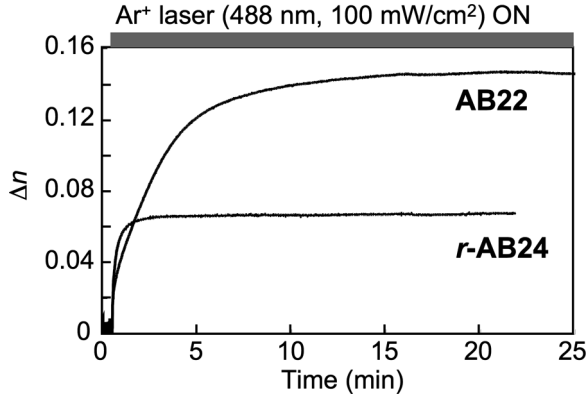

FIGURE 6 Photoinduced birefringence of **AB22** and ***r*-AB24** in film.

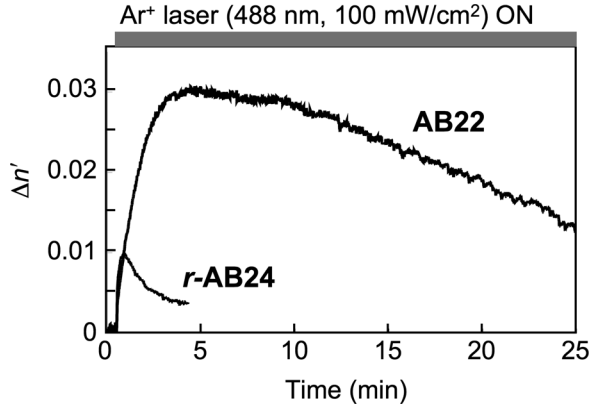

FIGURE 7 Modulation of refractive index of **AB22** and ***r*-AB24** in film.

higher than that in the ***r*-AB24** film. These results agree with a tendency of Δn discussed above. Az alignment is enhanced by cooperative motion of LCs in the **AB22** film. Figure 8 gives the possible mechanism for the change in alignment of Az moieties in the block and random copolymer films.

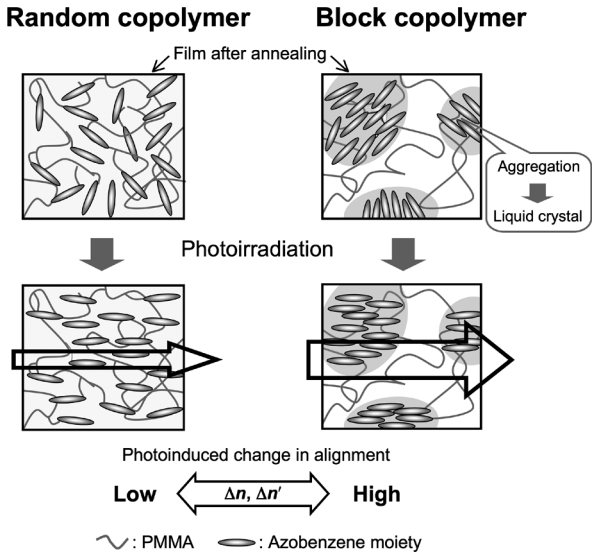

FIGURE 8 Schematic illustration of the Az-containing block copolymer and the random copolymer film before and after irradiation with a linearly polarized beam at 488 nm.

CONCLUSIONS

We prepared a **PMMA-Br** macroinitiator and a diblock copolymer with a low polydispersity by an ATRP method. The block copolymer with 22-mol% Az showed an LC phase, while a random copolymer with almost the same content of the Az moiety was amorphous. The photo and thermal isomerization in solution was fitted by the first-order plots. However, in annealed films, the degree of *trans-cis* photoisomerization was lower due to restricted motion of Az moieties. In particular, the degree of photoisomerization of the block copolymer was lower than that of the random copolymer.

In thin films, birefringence was generated upon irradiation with a linearly polarized beam. It was found that the modulation of refractive index ($\Delta n'$) between bright and dark fringes in **AB22** was four times higher than that in ***r*-AB24** thanks to the large anisotropy of LCs induced by photoirradiation. After annealing, Az moieties were homogenously dispersed in the random copolymer, while they formed microdomains in the block copolymer. Upon irradiation, a higher degree of alignment of Az moieties was obtained by the cooperative effect of LCs in the block copolymer films.

REFERENCES

[1] Ikeda, T. & Tsutsumi, O. (1995). *Science*, *268*, 1873.
[2] Ikeda, T. (2003). *J. Mater. Chem.*, *13*, 2037.
[3] Yamamoto, T., Hasegawa, M., Kanazawa, A., Shiono, T., & Ikeda, T. (2000). *J. Mater. Chem.*, *10*, 337.
[4] Eich, M. & Wendorff, J. H. (1987). *Makromol. Chem., Rapid Commun.*, *8*, 467.
[5] Saishoji, A., Sato, D., Shishido, A., & Ikeda, T. (2007). *Langmuir*, *23*, 320.
[6] Ishiguro, M., Sato, D., Shishido, A., & Ikeda, T. (2007). *Langmuir*, *23*, 332.
[7] Häckel, M., Kador, L., Kropp, D., & Schmidt, H. W. (2007). *Adv. Mater.*, *19*, 227.
[8] Breiner, T., Kreger, K., Hagen, R., Häckel, M., Kador, L., Müller, A. H. E., Kramer, E. J., & Schmidt, H. W. (2007). *Macromolecules*, *40*, 2100.
[9] Häckel, M., Kador, L., Kropp, D., Frenz, C., & Schmidt, H. W. (2005). *Adv. Funct. Mater.*, *15*, 1722.
[10] Tian, Y., Watanabe, K., Kong, X., Abe, J., & Iyoda, T. (2002). *Macromolecules*, *35*, 3739.
[11] Yu, H. F., Okano, K., Shishido, A., Ikeda, T., Kamata, K., Komura, M., & Iyoda, T. (2006). *Adv. Mater.*, *17*, 2184.
[12] Yu, H. F., Shishido, A., Li, J., Kamata, K., Iyoda, T., & Ikeda, T. (2007). *J. Mater. Chem.*, *17*, 3485.
[13] Yu, H. F., Asaoka, S., Shishido, A., Iyoda, T., & Ikeda, T. (2007). *Small*, *3*, 768.
[14] Yu, H. F., Shishido, A., Iyoda, T., & Ikeda, T. (2007). *Macromol. Rapid Commun.*, *28*, 927.
[15] Yu, H. F., Iyoda, T., & Ikeda, T. (2006). *J. Am. Chem. Soc.*, *128*, 11010.
[16] Frenz, C., Fuchs, A., Schmidt, H. W., Theissen, U., & Haarer, D. (2004). *Macromol. Chem. Phys.*, *205*, 1246.

[17] Moriya, K., Seki, T., Nakagawa, M., Mao, G., & Ober, C. K. (2000). *Macromol. Rapid Commun.*, *21*, 1309.
[18] Kadota, S., Aoki, K., Nagano, S., & Seki, T. (2005). *J. Am. Chem. Soc.*, *127*, 8266.
[19] Tong, X., Cui, L., & Zhao, Y. (2004). *Macromolecules*, *37*, 3101.
[20] Cui, L. & Zhao, Y. (2003). *Macromolecules*, *36*, 8246.
[21] Morikawa, Y., Nagano, S., Watanabe, K., Kamata, K., Iyoda, T., & Seki, T. (2006). *Adv. Mater.*, *18*, 883.
[22] Minabe, J., Maruyama, T., Yasuda, S., Kawano K., Hayashi, K., & Ogasawara, Y. (2004). *Jpn. J. Appl. Phys.*, *43*, 4964.
[23] Watanabe, K., Tian, Y., Yoshida, H., & Iyoda, T. (2003). *Trans. Mater. Res. Soc. Jpn.*, *28*, 553.
[24] Fisher, E. (1967). *J. Phys. Chem.*, *71*, 3704.
[25] Okano, K., Shishido, A., & Ikeda, T. (2006). *Macromolecules*, *39*, 145.
[26] Mita, I., Horie, K., & Hirao, K. (1989). *Macromolecules*, *22*, 558.
[27] Eisenbach, C. D. (1980). *Ber. Bunsen-Ges. Phys. Chem.*, *84*, 680.
[28] Barrett, C., Natansohn, A., & Rochon, P. (1994). *Macromolecules*, *27*, 4781.
[29] Paik, C. S. & Morawetz, H. (1972). *Macromolecules*, *5*, 171.